



THE MEASUREMENT OF THE ACOUSTIC PARTICLE VELOCITIES AND THE ACOUSTIC STREAMING VELOCITIES IN THE NEAR FIELD OUTWARD OF THE DUCT OPEN END USING PARTICLE IMAGING VELOCIMETRY TECHNIQUE

^{1,2} Neodir José Comunello

¹Instituto Tecnológico de Aeronáutica, Departamento de Propulsão. Pça Mal. Eduardo Gomes, 50
São José dos Campos, SP, Brasil, 12228-900

²Agência Nacional de Aviação Civil, Avenida Cassiano Ricardo, 521
São José dos Campos, SP, Brasil, 12246-870
neodir.comunello@anac.gov.br

Cristiane Aparecida Martins

Instituto Tecnológico de Aeronáutica, Departamento de Propulsão. Pça Mal. Eduardo Gomes, 50
São José dos Campos, SP, Brasil, 12228-900
cmartins@ita.br

Pedro Teixeira Lacava

Instituto Tecnológico de Aeronáutica, Departamento de Propulsão. Pça Mal. Eduardo Gomes, 50
São José dos Campos, SP, Brasil, 12228-900
placava@ita.br

Abstract. *This work presents how measurements of acoustic particle velocities and acoustic streaming velocities nearby the exit of a duct provided with acoustic actuation can be performed using particle imaging velocimetry (PIV) technique. A probabilistic method is used to figure out these velocities considering fact that the acquisition rate of the PIV equipment used is much smaller than the acoustic wave frequency. Frequencies tested are in the range of 50 up to 170 Hz, which includes the fundamental resonance frequency of the duct and forced oscillation. In this investigation region the acoustic waves that were plane waves just before the duct exit are spread out in spherical waves; in addition the resonance harmonics frequencies becomes more relevant in the total acoustic pressure outside when compared with their contribution inside de duct, this observation motivated a development of the probabilistic method to measure the acoustic particle velocity in acoustic chords. A non linear flow behavior is analyzed due to the asymmetry of the air flowing out the duct in relation to the air flowing into the duct during the acoustic oscillation cycle; this mechanism generates the streaming motions observed in the experience. It is disclosed the critical Strouhal number above which this kind of acoustic streaming is absent. The experimental results are confronted with acoustic and acoustic streaming theories predictions in the near field of the duct outlet, the conclusions shows the good reliability of the PIV technique and bring same light to explain when the acoustic actuation in flames are beneficial to reduce the flame length and pollutants emissions.*

Keywords: *combustion, PIV, acoustic particle velocity, acoustic streaming velocity*

1. Introduction

Tyndall (1970) indicated Higgins (1777) as the first person to figuring out the effects of acoustic waves over the behavior of flames. This event had occurred almost one century before Lord Rayleigh studies (1878). After that, innumerable studies have been done in different experimental configurations, always trying to relate sound and combustion. In fact, thermoacoustic instabilities have been target of attention for two chief reasons. The first is that some studies declared that thermoacoustic instabilities decrease or even increase pollutants (Kelly (1991), Martins et al. (2006), Keller et al. (1994)). The second is that in order to decrease pollutants, particularly NO_x sometimes is necessary the operating in conditions which are totally favorable to presence of the instabilities, lean premixed combustion. Recently, for example, one European project (2002-2006) called DESIRE (Design and demonstration of highly reliable low NO_x combustion systems for gas turbines) had as primary objective to provide models for predicting the interaction between the sound produced by the flame and the resulting vibrations of the liner of gas turbine (Kampen, 2006).

Thus, is very important the knowledge about interaction between sound and combustion. Clearly this involves measurements of the acoustics streaming. The former work submitted by Comunello et al. (2013) studies the behavior inside of the duct, the major part of the acoustical energy remains inside the duct and a small part of the energy leaks though the open end. One consequence of this is that, outside the duct, the input frequency loses its predominance in the acoustic pressure and particle velocity, what calls for an analysis of acoustic chords.

Comunello, N. J., Martins, C. A. and Lacava P.T.,
Acoustic Velocities in the Near Field Outside a Rectangular Duct using PIV

In the present work the acoustic particle velocity is investigated in the free space nearby the duct open end. The experimental assembly was complemented to measure the acoustic pressure outside the duct. In the methodology section at first it is exposed the iterative process used to figure out the acoustic particle velocities using particle imaging velocimetry (PIV) technique; afterwards the theoretical acoustic is called to help the underrating of the waves motion. The acoustic streaming herein studied is analyzed in its causes and some predictions are made based in the recent work of Grushin *et al.* (2001). The experiences results showed a good agreement with the theory prediction and the relevance of the prediction to distinguish among the experience data what is related to the kind of acoustic streaming. Figure 1 shows one example of the velocity field out of the duct.

It is possible to note that when the air flow is coming in the duct open end a point placed in the duct's centerline in the height position about -30 mm in the "Fig. 1" shows a changing on the velocity direction, which means that only the air below this position is traveling in the duct direction added by the surrounding air nearby the duct open end; while the air above this position is still traveling in the out flow direction. This position is about the same where the acoustic streaming achieves its maximum. When the air flow comes out of the duct the streamlines resembles an air jet as showed in the "Fig 2".

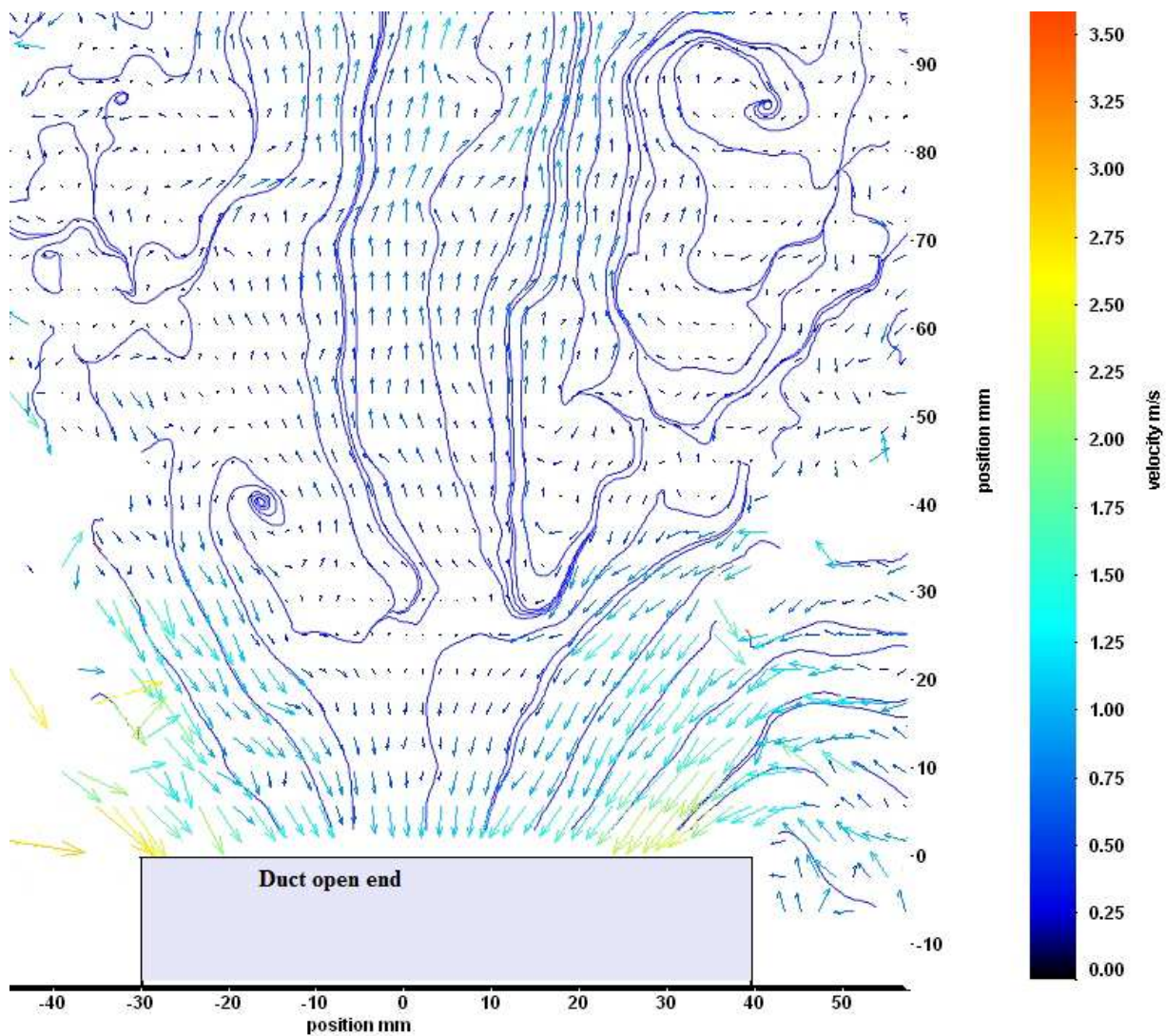


Figure 1: Image of the velocity field outward the duct open end when the air flow is coming in the duct open end. Arrow's lengths are proportional to the velocity and streamlines are showed as continuous lines.

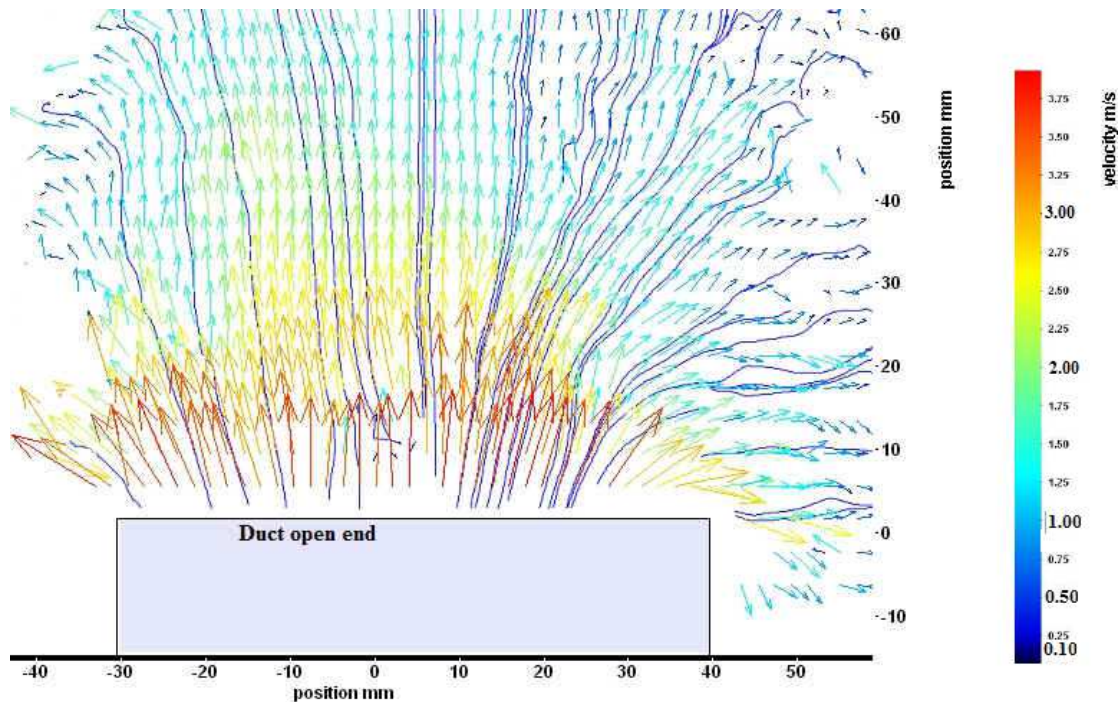


Figure 2: Image of the velocity field outward the duct open end when the air flow is coming out the duct open end.

2. DESCRIPTION OF THE EXPERIMENTAL ASSEMBLY

The basic experimental assembly was the same as constructed and reported in the work Comunello *et al.* (2013); the difference is the addition of the means to support the pressure sensor in the investigation region as showed in the “Fig. 3”. This was done using a photographic camera tripod that enables the positioning of the pressure sensor; the unique modification was an additional brace between the tripod and the pressure sensor in order to reach the right height and to fix the pressure sensor.

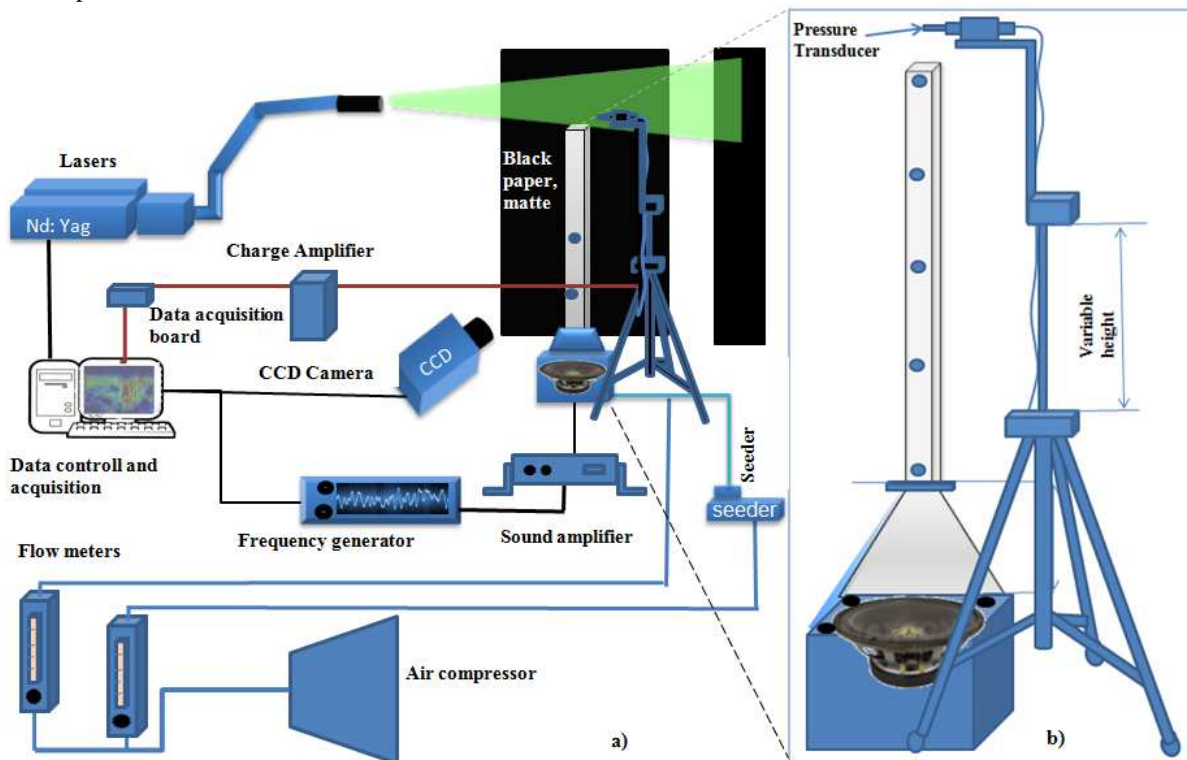


Figure 3. a) General assembly and b) Main duct assembly with additional support to measure the acoustic pressure nearby the open end.

3. METODOLOGY

3.1 Experimental PIV fundamental procedures

The proper adoption of the time between images “dt” is fundamental to get fine measurements of the velocity field. It is surprising that the proper choice of this variable depends on the acoustic particle velocity that will be measured, what suggest an iterative procedure. Without any other means of indirect velocity measurements about these values they may be chosen by a guess, in this experience the maximum acoustic pressure and the flow meter are used to infer the approximate particle acoustic and flow velocities to initiate the procedure. The following steps can be iteratively pursued:

First– Calculate the root mean square (rms) acoustic particle velocity, for this experience that the duct behaves as on open-open duct it can be figured out by theirs proportionally with the maximum acoustic pressure through the equation:

$$u'_{rms} = \frac{(p'_{rms})}{c\bar{\rho}} \quad (1)$$

Where c is the sound speed and $\bar{\rho}$ is the average mass density of the working fluid.

Second– Estimate the steady flow velocity $-\bar{u}$ - inside the duct can be assumed the flow is uniform along the cross section, therefore the simple relation between the air flux and the internal dimensions of the duct will point out the flow velocity.

Third – Calibrate, or get from the calibration, the conversion constant of pixels to meters ($cc_{p \rightarrow m}$)

Fourth- It is recommended to choice the interrogation window of 32x32 pixels, due the fact that it can be enlarged up to 128x128 pixels or reduced down to 8x8pixels, then calculate the interrogation windows side length (l_{int}) in meters by multiplying the calibration conversion value ($cc_{p \rightarrow m}$) by 32 (or other desired interrogation windows side)

Fifth – Calculate the “dt” range by the formula:

$$\frac{1}{4} \frac{l_{int}}{\bar{u} + u'_{rms}} \leq dt \leq \frac{1}{3} \frac{l_{int}}{\bar{u} + u'_{rms}} \quad (2)$$

Sixth – Chose an initial number of double images to be acquired, usually one hundred is enough for laminar plus acoustic waves flows, however it could be necessary up to one thousand for high turbulent flows.

Seventh - Proceed with the frames acquisition with a “dt” value set inside the range presented in the “Eq. 2”.

Note: Perform 3 or 4 pictures in the same conditions except the presence of the seed particles, this background pictures will be useful to subtract scattered light or other bright objects from the pictures with the seed particles before to run the PIV operations.

Eight– Before running PIV operations with the entire set, take just one sample of the double frames data and perform a correlation function, the result can be visualized in a correlation map. The height of each position is proportional to the multiplication of one intensity value with the other image intensity shifted on its position by all possible displacements, the highest position in the map indicates the more probable displacement. The image’s dominium is the interrogation window space. It is needs to range the interrogation window size until a clear peak appears, if is the case, in the correlation map. Examples of well defined and poor defined peaks in the correlation function are showed in “Fig. 4 a)” and “Fig. 4 b)” respectively. It should be noted that the correlation function is for a chosen interrogation window in the entire area of view, so it is recommended to perform this procedure in relevant regions where velocity wanted to be measured.

Ninth – Run PIV operations in the entire set using the chosen interrogation windows size and perform the post processing to extract the mean and rms particle velocities.

Tenth - With the rms particle acoustic velocities and flow velocities results return to the fifth step and refine de “dt” range. Modify the number images to be acquired in order to evaluated the change of the rms acoustic particle velocity until this value gets stable and keeping in mind that the PIV images files are heavy and the calculations time will be so large how much the images number to be processed.

The pictures quality plays a key role to achieve a fine velocity field measurement. The pictures quality control is performed ranging the focus and the light intensity while the resulting image in checked in the screen. The light intensity is controlled by the laser power setting and ranging diaphragm aperture.

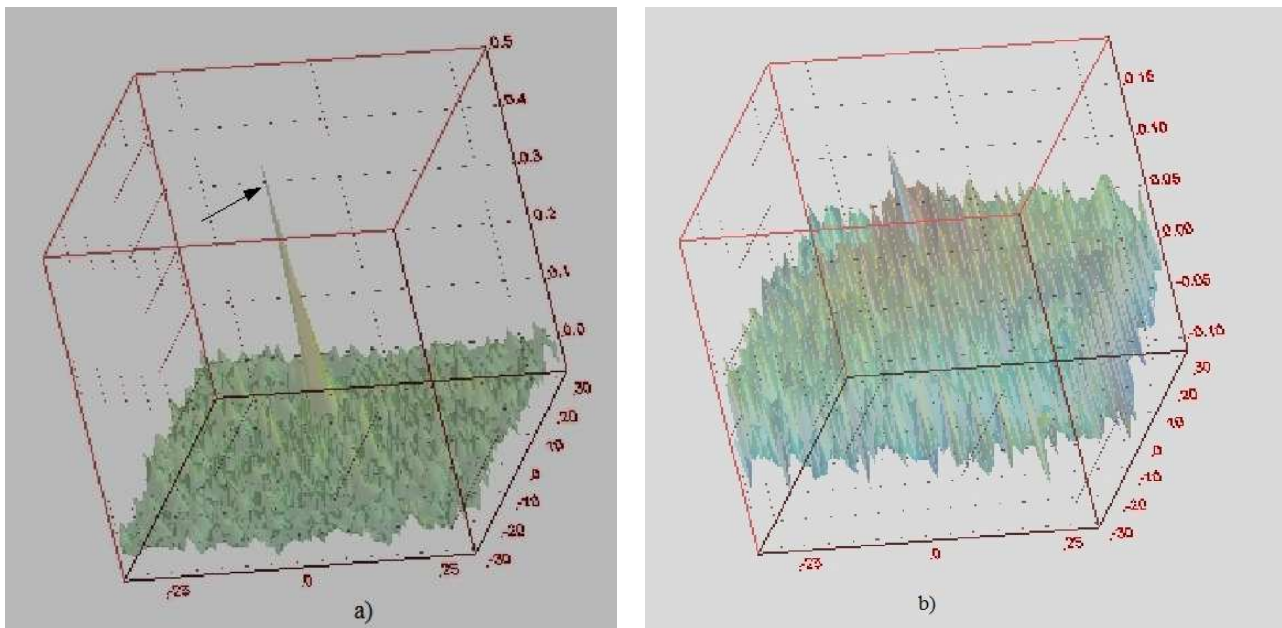


Figure 4. a) Correlation function with a well defined peak and b) Poor defined peaks in the correlation function

3.2 Treatment of the raw acoustic particles velocity measurements in chords

The treatment to the raw, or total, velocity measurement was done in a previous paper by Comunello *et al.* (2013) considering the case where the total velocity is compounded by a steady flow plus one predominant wave. In the present experiences where the free space nearby the duct open end is the investigation region it is foreseen that the predominance of one wave isn't the case, even in the resonance condition the great majority of the wave energy remains inside the duct while a little part of this energy leaks to the free space. The case of a chord, which is an acoustical wave compounded by two or more simple harmonic wave, the acoustic pressure and particle velocity relationship can be developed looking to the raw acoustic particle velocity as an interference result of two or more single acoustic waves.

At first each simple harmonic wave changes the way it moves when it passes at the duct open end from plane wave motion to a spherical like wave motion. Here will be used the imaginary piston of zero mass at the open end, as described by Morse and Ingard (1968), which radiates sound out into the free space as well as reflecting some back down to the duct. Now the part of the acoustic energy that radiates into the free space is the object; the boundary condition at the open end is without flange, what means that the sound must spread out over the whole solid angle of 4π . Since this piston is a square flat surface the actual wave front has an ellipsoid shape, however the assumption that the sound radiation will occur on spherical waves is simpler and will provide the right relationships of the wave motion in the duct centerline. In accordance with Morse and Ingard (1968) the relationship between acoustic pressure and velocity depends on the distance from the source to the measurement point r ; if r is large compared with the wavelength the sound field in this region is called the far field, where acoustic velocity is in phase with the acoustic pressure and their relationship approaches the ones given for plane waves. In this experience the investigation region is the near field, if the characteristic length of the duct cross section is small compared with the wavelength, in the special case when the source is a simple harmonic the acoustic pressure wave at a distance r from the centre of the sphere is:

$$P'(r, t) = \frac{-ik\bar{\rho}c}{4\pi r} S_w e^{ik(r-ct)} \quad k = \frac{w}{c} = \frac{2\pi}{\lambda} \quad (3)$$

Where k is the wave number; w the angular velocity; c is the sound speed in the medium, $\bar{\rho}$ is the average medium density, λ is the wavelength, i is the imaginary number and S_w is the source strength defined as:

$$S_w = 4\pi r_0^2 u'_{0 \max} \quad (4)$$

Where r_0 is the sphere radius and $u'_{0 \max}$ is the maximum acoustic velocity at the sphere surface.

It is needed to convert this ideal spherical condition to the actual condition of a piston at the duct open end; this can be done converting the open end cross section area in an equivalent sphere with the same surface area by:

Comunello, N. J., Martins, C. A. and Lacava P.T.,
Acoustic Velocities in the Near Field Outside a Rectangular Duct using PIV

$$4\pi r_0^2 = a^2 \Leftrightarrow r_0 = \sqrt{\frac{a^2}{4\pi}} \quad (5)$$

Where r_0 is the equivalent sphere radius and a is the side length of the square section of the duct.

Substituting “Eq. 5” in the “Eq. 4” and afterwards in the “Eq. 3” and changing the reference from the sphere centre to the duct open the real part of acoustic pressure can be written as:

$$P'(x, t) = \frac{\bar{p}c}{2\lambda\left(x + \sqrt{\frac{a^2}{4\pi}}\right)} a^2 u'_{0 \max} \left(\text{sen} \frac{2\pi}{\lambda} \left(x + \sqrt{\frac{a^2}{4\pi}} \right) \cos \omega t - \cos \frac{2\pi}{\lambda} \left(x + \sqrt{\frac{a^2}{4\pi}} \right) \text{sen} \omega t \right) \quad (6)$$

Where x is the distance from the duct open end section center to the measurement point.

The root mean square acoustic pressure is measured by:

$$(P'_{rms}(x))^2 = E[P'(x, t)^2] = \frac{1}{2} \left(\frac{\bar{p}c}{2\lambda\left(x + \sqrt{\frac{a^2}{4\pi}}\right)} a^2 u'_{0 \max} \right)^2 \quad (7)$$

To an acoustic chord compounded by n relevant waves the total rms pressure will follow the equation:

$$(P'_{t \text{ rms}})^2 = \sum_{i=1}^n (P'_{i \text{ rms}})^2 \quad (8)$$

The acoustic velocity has only the radial component, with a large component out of phase with the acoustic pressure in the near field, figured out by:

$$u'(x, t) = \frac{P'(x, t)}{\bar{p}c} \left(1 + \frac{i\lambda}{2\pi\left(x + \sqrt{\frac{a^2}{4\pi}}\right)} \right) \quad (9)$$

The root mean square acoustic particle velocity is:

$$(u'_{rms}(x))^2 = \frac{1}{2} \left(\frac{1}{2\lambda\left(x + \sqrt{\frac{a^2}{4\pi}}\right)} a^2 u'_{0 \max} \right)^2 + \frac{1}{2} \left(\frac{1}{4\pi\left(x + \sqrt{\frac{a^2}{4\pi}}\right)^2} a^2 u'_{0 \max} \right)^2 \quad (10)$$

The total rms acoustic particle velocity is developed in a similar rationale to keep the relationship:

$$u'_{t \text{ rms}} = \sqrt{\sum_{i=1}^n (u'_{i \text{ rms}})^2} \quad (11)$$

Figure 5 presents the rms acoustic pressures measured after an input frequency of 161 Hz in the loudspeaker; in parallel it is showed the acoustic pressures calculated by “Eq. 7” for individual waves and “Eq. 8” for the acoustic chord; afterwards the rms acoustic particle velocities components are inferred by the proper equations. It is notable that the velocities components that are out of phase with the pressure dominate the total rms acoustic particle velocity in the near field. It is relevant to point out that in the near field the acoustic **pressure** presents the decay shape inversely proportional to the distance from the duct’s open end while the acoustic particle **velocity** presents the decay shape inversely proportional to the square of the distance from the duct’s open.

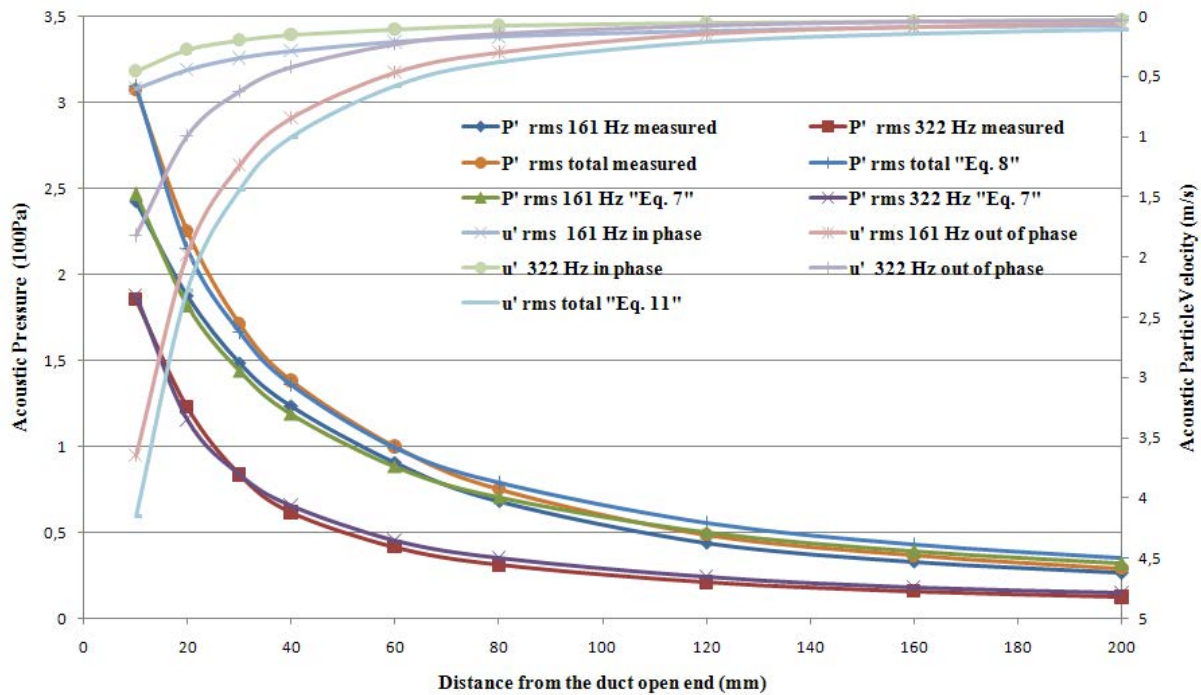


Figure 5. Acoustic chord pressure and velocity decay obtained from an input frequency of 161 Hz (the frequency resonance of the duct). Note the acoustic velocity axis is inverted to enhance the figure visualization.

The flow and the rms acoustic particle velocities will be figured out by the mean and the standard deviation of the raw velocities readings using the PIV technique.

3.3 The cause and the relationships of the acoustic particle streaming in the near field outward of the duct open end

The acoustic streaming formed outward of the duct open end is related to the nonlinear behavior caused by the edges at the duct open end within each oscillation cycle. In the work of Lebedeva and Grushin (2003) it is recognized that this kind of acoustic streaming “differs essentially on a well-known Rayleigh, Eckart and Schlichting streams in liquid, whose particle velocities are an order of magnitude smaller than the acoustic velocity”. The nonlinear behavior is related to the different qualities of the near field flows coming out and coming in through the open end, i.e., when the air flow comes out of the duct its separation from the sharp edges of the opening gives rises to vortices; when the air flow changes the direction the surrounding medium flows into the duct without vortices formation as showed in “Fig.1” and “Fig.2”. The authors of the above paper developed a method to measure the acoustic streaming formed outward of the duct open end of the duct at its resonance frequency, it was used the hot-wire anemometer technique to register the streaming and the oscillating part of the velocity field. The results presented showed that at the open cross section the acoustic streaming velocity is null, advancing in the duct centerline up to the distance of 1.3 times the duct diameter it increases close to linearity and reaches the order of the amplitude of the acoustic particle velocity at the open end; beyond this maximum there is a region of stabilization up to 2 times the duct diameter and afterwards it decreases quite linearly depending on the frequency. The typical evolution for 175 Hz in the cited experience, where the duct is round and its diameter is 0.0235 m, may be represented by:

$$\frac{\bar{u}'_{as}}{u'_{01\max}} \cong \begin{cases} \frac{x}{1.3l_{01}} \quad \forall x \in [0; 1.3l_{01}] \text{ region 1} \\ 1 \quad \forall x \in [1.3l_{01}; 2l_{01}] \text{ region 2} \\ \frac{10}{9} - \frac{x}{12l_{01}} \quad \forall x > 2l_{01} \text{ region 3} \end{cases} \quad (12)$$

Where \bar{u}'_{as} is the acoustic streaming velocity; $u'_{01\max}$ is the amplitude of the oscillating acoustic particle velocity at the duct open end, x is the distance from the open end to the measurement point along the duct centerline and l_{01} is the characteristic length of the duct open end cross section.

To be able to compare this result with other experiences it is needed to refer to the same Strouhal number, which is defined by:

Comunello, N. J., Martins, C. A. and Lacava P.T.,
Acoustic Velocities in the Near Field Outside a Rectangular Duct using PIV

$$St = \frac{f_0 l_0}{u'_{0 \max}}; St_{\text{exp}1} = St_{\text{base}} \Leftrightarrow u'_{01 \max} = u'_{0 \max} \frac{f_1 l_{01}}{f_0 l_0} \tag{13}$$

Where $u'_{0 \max}$, f_0 and l_0 are the amplitude of the oscillating acoustic particle velocity, the wave frequency and the characteristic length of the duct outlet cross section in a base experience, respectively.

Therefore the representative “Eq. 12” obtained from the work of Lebedeva and Grushin (2003) should be mapped to this experience, with includes the regions limits, by the following equation:

$$\left(\frac{\bar{u}'_{as}}{u'_{0 \max}}\right)_{\text{based at } f_0 \text{ and } l_0} = \begin{cases} \frac{f_1}{f_2} \frac{x}{1.3 l_0} \quad \forall x \in \left[0; 1.3 \frac{l_{01}}{l_0}\right] \\ \frac{f_1}{f_2} \frac{l_{01}}{l_0} \quad \forall x \in \left[1.3 \frac{l_{01}}{l_0}; 2 \frac{l_{01}}{l_0}\right] \\ \frac{10}{9} \frac{f_1}{f_2} \frac{l_{01}}{l_0} - \frac{f_1}{f_2} \frac{x}{12 l_0} \quad \forall x > 2 l_{01} \end{cases} \tag{14}$$

The measurements of this experience performed with different frequencies, although the duct outlet geometry is the same, can be related to the base per:

$$\left(\frac{\bar{u}'_{as}}{u'_{0 \max}}\right)_{\text{based at } f_0} = \frac{f_1}{f_0} \left(\frac{\bar{u}'_{as}}{u'_{01 \max}}\right)_{\text{measured at } f_1} \tag{15}$$

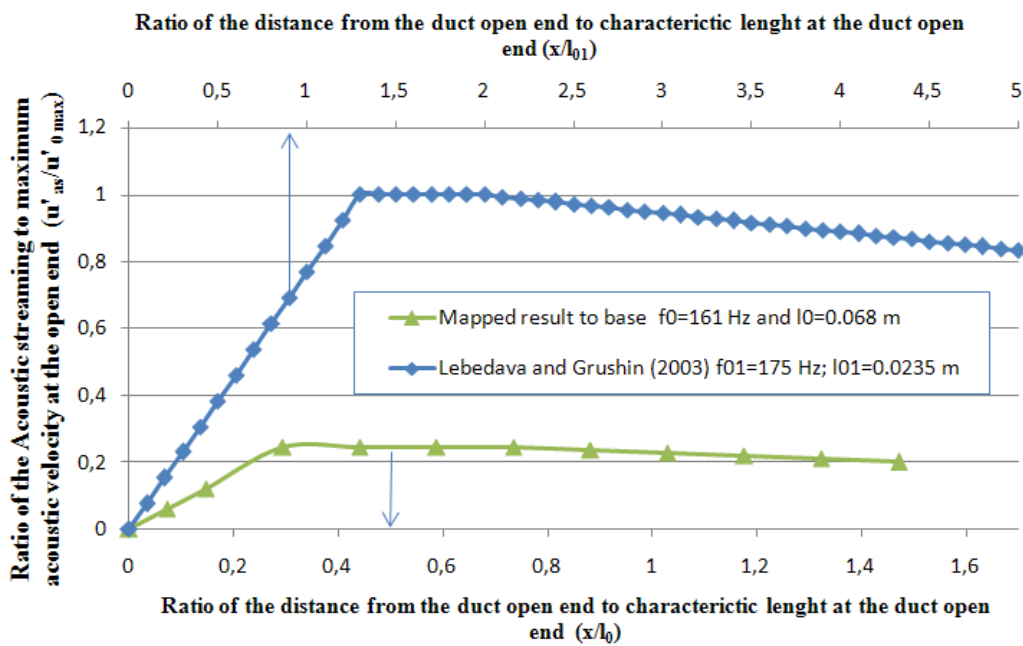


Figure 6. Typical evolution of the acoustic streaming velocity with the position along the duct centerline and its map for future comparison with experience at 161 Hz and $l_0=0.068$ m

Additional results of the work of Lebedeva and Grushin (2003) showed that there is an amplitude threshold value of the acoustic particle velocity at the open end above which the acoustic streaming emerges and that this critical acoustic velocity depends on the frequency. Analyzing the amplitude values of the critical acoustic velocities at the open end versus the frequencies tested it is notable that the ratio between the frequency and the critical acoustic velocity is quite constant. Since the duct’s geometry was the same in all tests then it is correct to put the hypothesis that the critical acoustic velocity amplitude threshold is related to the Strouhal number, this conjecture is reinforced taking into consideration the work of Crown and Champagne (1971), where the changes in the structure of the jet turbulence are related to the Strouhal number. Applying the “Eq. 13” for the results showed by Lebedeva and Grushin (2003), where the duct open end characteristic length is the tube diameter and there is no flow velocity, the critical Strouhal number above which this kind of acoustic streaming is absent is about 1.7.

It is questionable if the r.m.s flow velocity caused by the vortices in the investigated region may affect the measurements attributed to r.m.s acoustic velocity; however consulting the work of Crown and Champagne (1971) it is showed that up to the distance of 5 times the duct outlet diameter from the duct open the rms the velocity related to turbulent motion is less than 5% of the velocity at the duct open end, therefore is this experience the rms turbulent velocity was considered irrelevant to contribute to the raw rms velocity reading.

4. EXPERIENCE'S RESULTS AND DISCUSSION

The test conditions at the duct open end are showed in the "Tab. 1". The average flow velocity is kept at a minimum just to fulfill the investigation region with the seed particle and then highlight the acoustic actuation consequences in the fluid dynamics. The input voltage to the loudspeaker was constant at $14.8 V_{rms}$.

Table 1. Test conditions to measure the acoustic particle velocity and acoustic streaming

Input Frequency (Hz)	Duct open end characteristic length (m)	Acoustic particle velocity amplitude at duct open end (m/s)	Flow velocity at duct open end (m/s)	Strouhal number
161	0.068	13.25	Close to null	0.826
100	0.068	2.00	Close to null	3.4

The rise of harmonics of the fundamental frequency (f_0) may be seen as a strategy of the assembly to keep exceeding energy in other levels of frequency; in the conditions tested herein it is notable that inside the duct the preferred modes are the odd multiples of the fundamental frequency ($3f_0, 5f_0, \dots$) while outwards the duct open end the harmonics follows the natural sequence ($2f_0, 3f_0, \dots$). Probably it is due the boundary conditions imposed by the assembly inside the duct while there are no restrictions in the free space outside the duct.

The measured acoustic pressures outside the duct showed some frequencies added to the input frequency with similar amplitudes, the amplitude of the input frequency is in the order a tenth of its maximum observed inside the duct. When the input frequency is out of the resonance frequency as showed in the "Fig. 7" the number of waves in the acoustic chord outside the duct is bigger than when the input frequency matches the resonance frequency, as showed in "Fig. 8". Even when the input frequency doesn't match the resonance frequencies the resonance wave and its harmonics are excited.

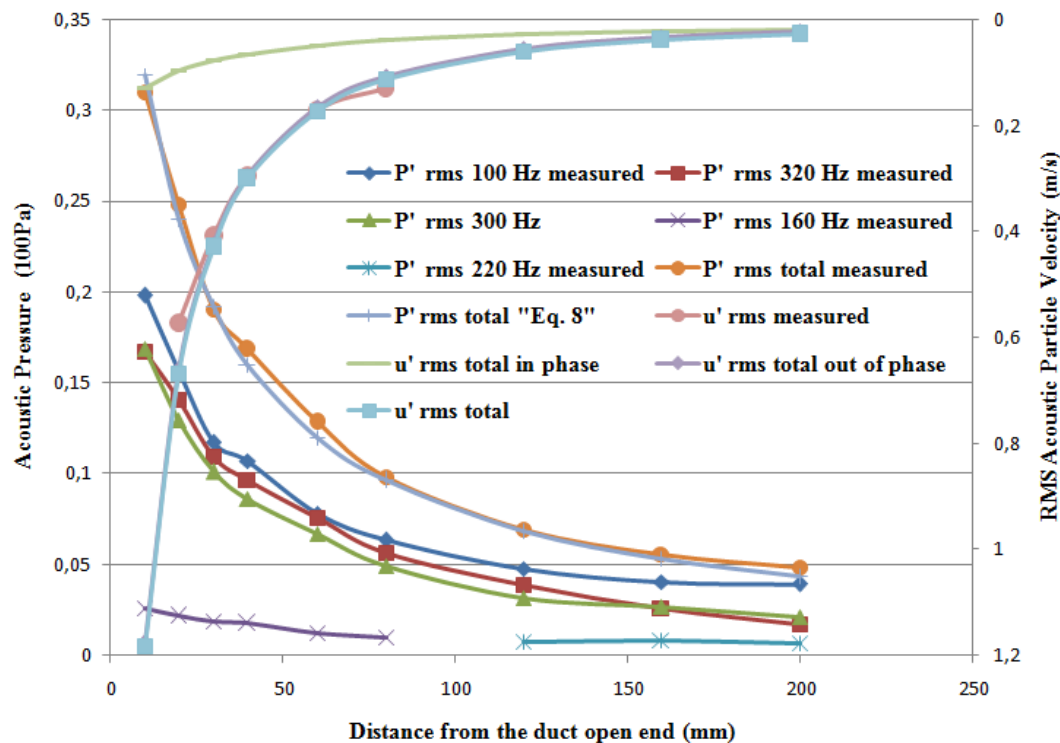


Figure 7. Acoustic pressure composition nearby the duct open end outside to input frequency of 100 Hz

The decay of the acoustic pressure and the acoustic particle velocities outwards the duct open end are very close of the predicted ones in the methodology chapter for spherical spread out of the sound.

Comunello, N. J., Martins, C. A. and Lacava P.T.,
Acoustic Velocities in the Near Field Outside a Rectangular Duct using PIV

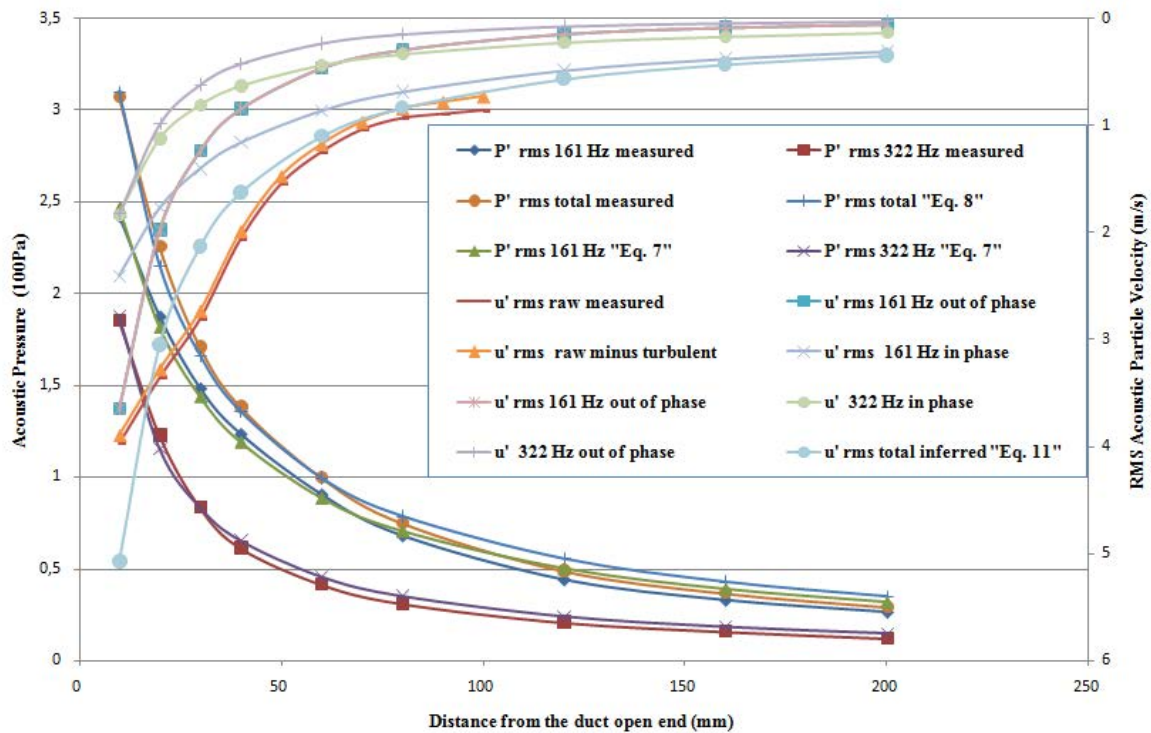


Figure 8. Acoustic pressure composition nearby the duct open end outside to input frequency of 161 Hz

The acoustic streaming velocities results based at $f_0 = 161$ Hz and duct outlet characteristic length of $l_0 = 0.068$ m, presented in the “Fig. 9”, showed that for the input frequency of 161 Hz the evolution in the space is similar, what confirms that the cause of the acoustic streaming observed in this experience are the non linear behavior explained in the methodology chapter. However the results of the acoustic streaming for input frequency of 100 Hz are dissimilar in its evolution in space and taking into consideration the critical Strouhal number of 1.7 which is exceeded in the test it is concluded that the streaming observed can not be related to the acoustic streaming herein discussed. The small velocities detected, in the order of the 0.5 m/s, are likely related to flow velocity.

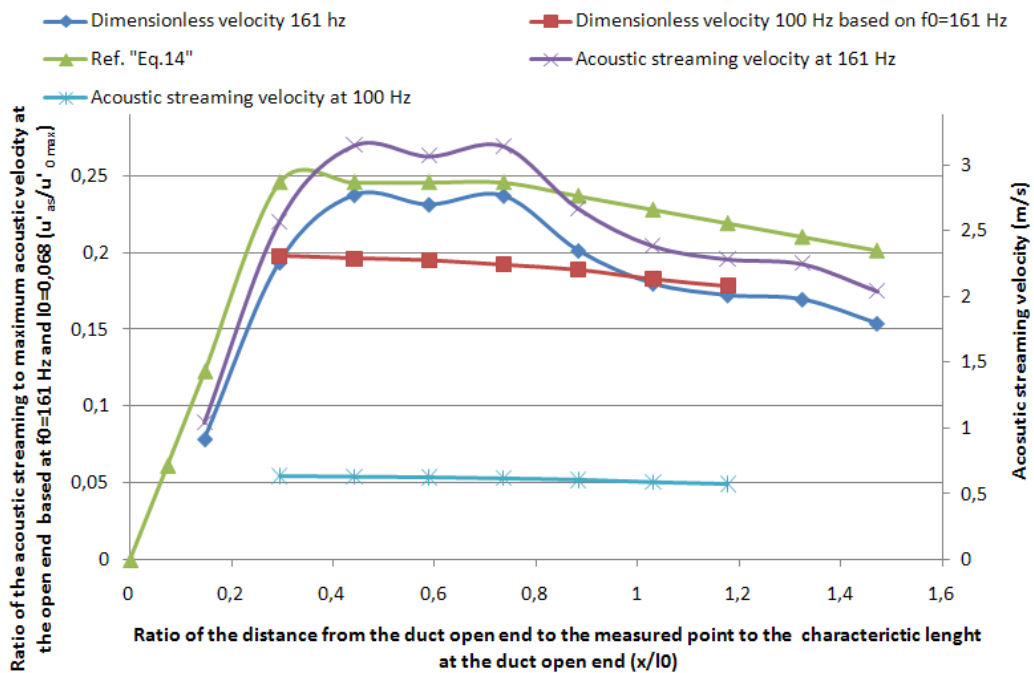


Figure 9. Typical shape of the acoustic streaming velocity in the near field outwards the duct open end and the results of the experience.

22nd International Congress of Mechanical Engineering (COBEM 2013)
November 3-7, 2013, Ribeirão Preto, SP, Brazil

5. CONCLUSIONS

The main achievements of this paper can be summarized as:

- There is a large component of the acoustic particle velocity in the near field outwards the duct open end which is out phase with the acoustic pressure. This components decays abruptly in space; the results confirms the sentence that the in the near field the pressure decays proportionally to the inverse of the distance of the measurement point to the duct open end cross section while the acoustic particle velocity decays proportionally the square of this distance.
- It is disclose from the paper of Lebedeva and Grushin (2003) the critical Strouhal number of about 1.7, below which this kind of acoustic streaming is present. This conclusion reinforces and explains the mechanism responsible to reduce the pollutant emission and reduce the flame length when the input frequency is close to the resonance frequency of the duct assembly.
- The acoustic streaming evolution in space present a typical shape as showed in the “Fig. 9”. This typical shape can be helpful to distinguish the streaming which is related to the acoustic actuation and other kinds of streaming.

6. REFERENCES

- Comunello, N.J., Martins C.A. and Lacava, P.T. (2013), “The measurement of the acoustic particle velocities inside a rectangular duct using particle imaging velocimetry technique”, ”, Proceedings of the 22th Brazilian Congress of Mechanical Engineering.
- Crown, S.C. and Champagne, F.H., 1971, “Orderly structure in jet turbulence”, *Journal of Fluid Mechanics*, Vol. 48, part 3, pp. 547-591.
- Grushin, A.E., Dragan, S.P. and Lebedeva L.V., 2001, “Dependence of the Acoustic Streaming on the Intensity of Sound in the Waveguide”, Proceedings of the XI Session of the Russian Acoustical Society, November 19-23, Moscow, Russia, pp. 286-288.
- Lebedeva, I. V.; Grushin, A. E (2003), Amplitude and Frequency Characteristics of Acoustic Jets, *Acoustical Physics*; May2003, Vol. 49 Issue 3, p300.
- Kampen J.F. (2006), *Acoustic Pressure Oscillations Induced by Confined Turbulent Premixed Natural Gas Flames*, PhD thesis, University of Twente, Enschede, The Netherlands, March 2006.
- Kelly, J., Woodworth, R., and Grant, C., Reducing Gas-Fired Pulse Combustor NO_x Emissions, Paper presented at the *International Symposium on Pulsating Combustion*, Monterey, CA, 1991.
- Keller, J.O., Bramlette, T.T., Barr, P.K., and Alvarez, J., NO_x and CO Emissions from a Pulse Combustor Operating in a Lean Premixed Mode, *Combustion and Flame* 99:460-466, 1994.
- Martins, C. A. ; Ferreira, M. A. ; Veras, C. A. G. ; Lacava, P. T. ; Carvalho JR, J. A. (2006). Experimental Measurements of the NO_x and CO Concentrations Operating in Oscillatory and Non-oscillatory Burning Conditions. *Fuel* (Guildford) , USA, v. 85, p. 84-93.
- Morse, P.M. and Ingard, K.U., 1968, “Theoretical Acoustic”, McGraw-Hill Book Company, New York, NY, USA.
- Tyndall, J., *J. Physical Sciences* 2:30-37, 1970.

7. RESPONSIBILITY NOTICE

The authors are the only responsible for the printed material included in this paper.